Photonic-Molecule Single-Mode Laser

Jin-Feng Ku, Qi-Dai Chen, Xiu-Wen Ma, Yue-De Yang, Yong-Zhen Huang, *Senior Member, IEEE*, Huai-Liang Xu, and Hong-Bo Sun, *Member, IEEE*

***Abstract*— We report in this letter the fabrication of edge-alignment-coupled whispering gallery mode photonic-molecule microdisk by femtosecond laser direct writing of dye-doped resins, which results in single-mode lasing output. Under picosecond laser pumping, the excited energy is distributed at the disk periphery and the coupling happens at the overlapping edge of two disks. As a result of mode coupling through Vernier effect, single-mode lasing is achieved in two-microdisk and three-microdisk coupled lasers of various sizes. The effect in the coupled system is confirmed by numerical simulation. This letter may open up a new avenue to the 3-D integrated optoelectronics.**

***Index Terms*— Whispering gallery mode (WGM), microcavity, single mode lasing, Vernier effect.**

I. Introduction

WHEN light travels at the periphery of a cavity by total internal reflection (TIR), standing wave oscillation can be formed when the optical path meets an integer multiple of the wavelength. It results in equally spaced discrete resonant mode which is usually called whispering gallery mode (WGM) [1]–[6]. WGM microcavities such as microdisk, microring and microtoroid have attracted much attention in applications of biosensing [7], microlaser [8], nonlinear optics [9] in the last decades because of their small mode volume and ultrahigh quality factor (Q-factor) that can be up to 10^{10}. Since single-mode microcavity lasers have great potential applications in optical communication, biochemical sensing, spectroscopy etc. [10], many methods have been proposed to achieve single mode lasing. For example, one efficient way is to reduce the size of the cavity so that the free spectral range (FSR) can be increased significantly. However, this results in the low Q-factor [11] making it impractical for many applications that require high Q factors such as optical storage, high speed all optical switches, electro-optic modulator. The alternative method to generate the single-mode lasing is to employ coupled WGM microcavities [12]–[14]. For instance, the coupled fiber lasers [14]–[16] with single-mode output have been demonstrated. However the coupled fiber lasers have a large mode volume and footprint. In this Letter, we report realization of single-mode polymer photonic-molecule (PM) microdisk laser fabricated by femtosecond laser direct writing (FsLDW) via two-photon photopolymerization of Rhodamine B (RhB) doped epoxy-based negative resin SU-8.

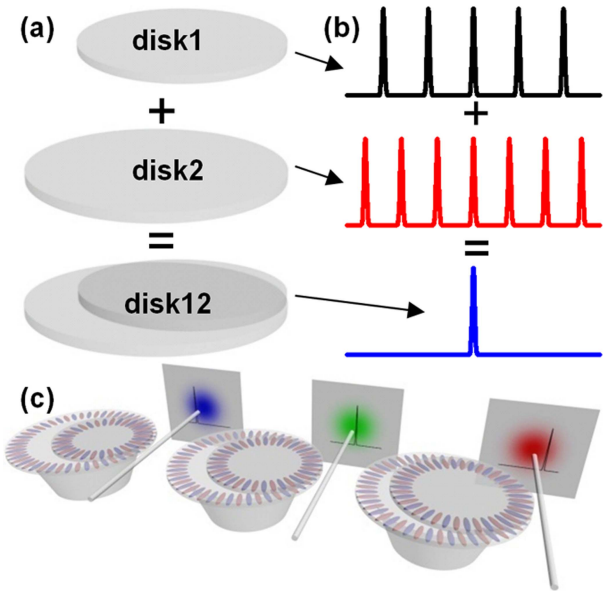

Fig. 1. The structure of the polymer PM single-mode laser. (a) The schematic diagram of the two microdisks coupled laser. (b) The principle of the single-mode laser with Vernier effect. (c) Three lasers are shown. By simply changing a small smout of size, temperature etc, the lasing wavelength can be modulated in a wide range.

II. Theory and Experiments

For a single disk (e.g. disk1 or disk2) shown in Fig. 1(a), many WGMs with different azimuthal numbers can be excited at the periphery of the disk (see Fig. 1(b)). Since disks with different diameters have different FSR, if two disks with different diameters are stacked together with edge alignment (see disk12), the stacked disk12 may lead to the resonance of some lasing modes to achieve single-mode lasing (Fig. 1(b)). When the free spectral range (FSR) of the small and the large disks are FSR_1 and FSR_2 respectively, the FSR for the PM laser (FSR_{12}) can be calculated as $FSR_{12} = N_1FSR_1 = N_2FSR_2$, where N_1 and N_2 are co-prime integers [14]. Therefore, these two coupled disks with different FSRs would suppress some resonances and make the effective FSR greatly increased, which has been described as the Vernier effect [12], [14]. With increased FSR, the coupled

Manuscript received December 15, 2014; revised March 4, 2015; accepted March 10, 2015. Date of publication March 16, 2015; date of current version May 8, 2015. This work was supported in part by the National Basic Research Program of China under Grants 2014CB921302 and 2011CB013003, and in part by in National Natural Science Foundation of China under Grants 61435005, 91423102, and 91323301.

J.-F. Ku, Q.-D. Chen, H.-L. Xu, and H.-B. Sun are with the State Key Laboratory on Integrated Optoelectronics, College of Electronic Science and Engineering, Jilin University, Changchun 130012, China (e-mail: chenqd@jlu.edu.cn; hbsun@jlu.edu.cn).

X.-W. Ma, Y.-D. Yang, and Y.-Z. Huang are with State Key Laboratory on Integrated Optoelectronics, Institute of Semiconductors, Chinese Academy of Sciences, Beijing 100089, China.

Color versions of one or more of the figures in this letter are available online at http://ieeexplore.ieee.org.

Digital Object Identifier 10.1109/LPT.2015.2413052

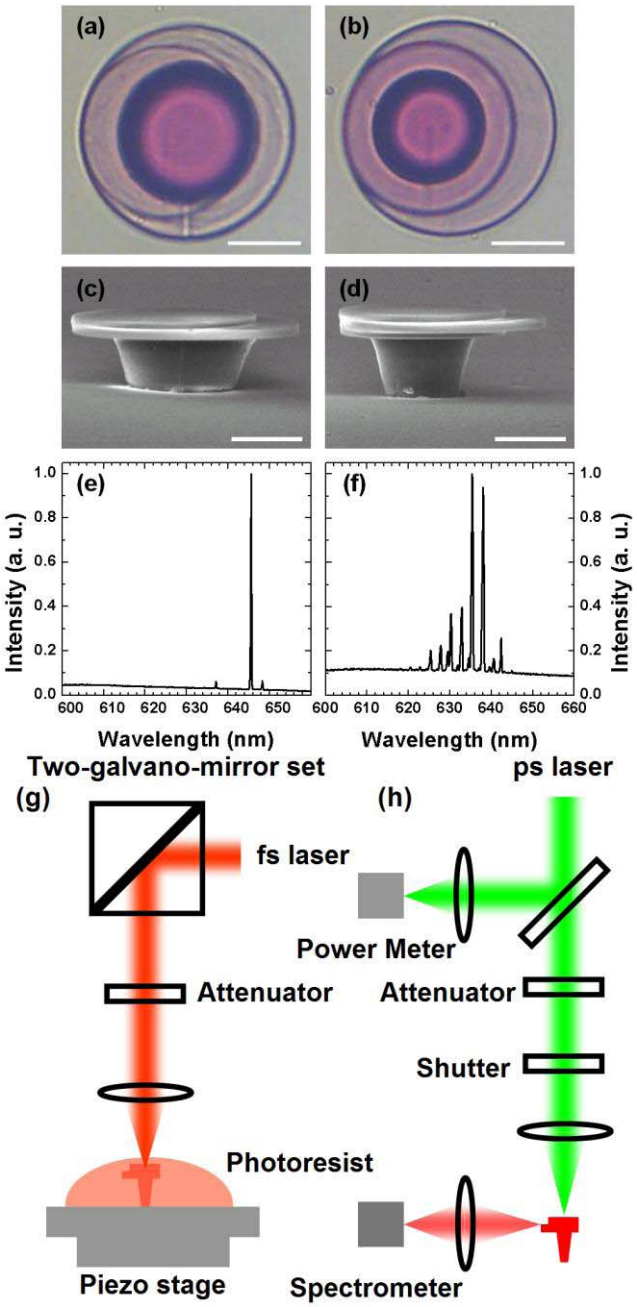

Fig. 2. Two microdisks coupled laser and three microdisks PM laser. (a) and (b) are optical microscopic images. (c) and (d) are SEM image respectively. The scale bars of (a)-(d) are 10 μm. (e) The spectrum of a three microdisks PM laser. (f) The spectrum of a single microdisk laser. (g) Schematic of femtosecond (fs) laser direct writing system. (h) Picosecond (ps) pumping and signal analysis system.

disks can exhibit single mode lasing in the gain region. In particular, slight variation of the cavity parameters such as the diameter, the reflective index of the surrounding medium can lead to a huge change in the on-resonance wavelength as shown in Fig. 1(c). This is extremely useful in the integrated optoelectronics.

The fabricated devices by FsLDW are shown in Fig. 2. The FsLDW fabrication process has been described elsewhere [17]–[20]. Briefly, pulses from a femtosecond laser oscillator (from Tsunami, Spectra Physics) with a central wavelength at 790 nm, a pulse width of 120 fs, and a repetition rate of 80 MHz were tightly focused by a high numerical aperture (NA = 1.35) 100× oil objective into epoxy-based negative resin SU-8 2025 (MicroChem) doped with Rhodamine B (RhB) with a concentration of ∼1 wt%. Before the fabrication, a soft-bake step was applied to the material for 2 hours at 95 °C in an oven. The laser focal spot was scanned point by point with the lateral dimensions by a two-galvano-mirror set and the lengthwise dimension by a piezo stage as shown in Fig.2 (g). Two-photon polymerization that guarantees the precision of the micro-nano-structure occurred at the focal spot. Laser power of 8-12 mW and exposure duration of 300 μs were adopted. After the fabrication, the resin was post-baked for 30 minutes at 95 °C, and finally developed in the acetone for 3 minutes.

Fig. 2 shows the top-view optical microscopic images and the side-view scanning electron microscope (SEM) images with different structures of two stacked microdisks (Figs. 2(a) and 2(c)) and three stacked microdisks (Figs. 2(b) and 2(d)). A cone-shape pedestal was fabricated to support the coupled disks in air making the reflective index difference between the PM disks and the surrounding medium large enough to support WGM lasing. As an example, the spectrum of three stacked microdisks with the diameters of 24 μm, 30 μm and 24 μm respectively is shown in Fig. 2(e), which obviously gives rise to single mode lasing, resulting from mode coupling between the microdisks (see later). To compare, the spectrum of a single disk with a diameter of 30 μm is shown in Fig. 2(f), in which more than eight modes from the cavity are generated.

It should be pointed out that the femtosecond laser direct writing technique was also used previously to fabricate micro-cavities [19], [20]. However, previous studies only focus on the fabrications of active single microdisk with multimode lasing [19] or of deformed passive single micordisk without lasing output [20]. Therefore, the coupled microdisks shown here provides insight into the understanding of the couping of multicavities by characterizing the single mode output of the microcavities fabricated by femtosecond laser direct writing.

III. Results and Disscussion

The Rhodamine B doped SU-8 has a wide absorption band from 520 to 580 nm and an emission band in the spectral range of 580-700 nm. Therefore, in this work, the coupled WGM microcavities were pumped from the top by a 532 nm (frequency doubled from a 1064 nm laser) picosecond (ps) laser with a pulse width of 15 ps, and a repetition rate of 50 KHz. A shutter with an opening time of 20 ms and a separation time of 1 minute is added in the light path in order to avoid the degradation of RhB doped in the microdisk. As a result, no degradation of the microcvatiy is observe under such experimental condition. In order to make a nearly homogeneous distribution of the intensity of the pump laser on the microcavities, a focal spot size of ∼200 μm, which is much larger than the microcavities, was used. A lens with a focal length of 50 mm was put beside the microcavtiy at 200 mm (see Fig. 2(h)). The emission light was collected by

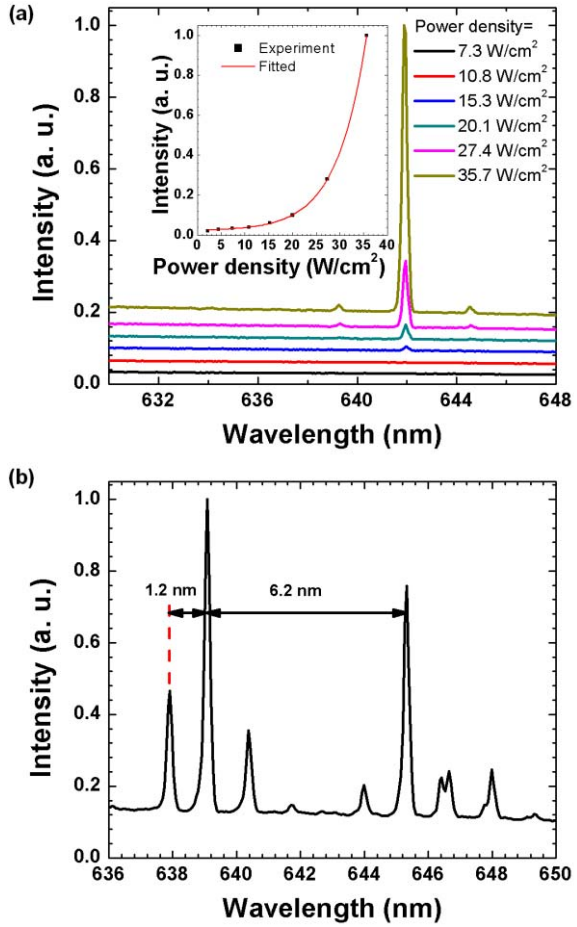

Fig. 3. The lasing spectrum of the single-mode PM laser. (a) The emission spectrum of two coupled microdisk lasers with diameter of 18 μm and 30 μm. The inset shows the light output versus the pumping intensity. (b) Spectrum with more modes is shown, indicating the Vernier effect.

a spectrometer equipped with a CCD (Charge coupled device) camera by setting the probe at the focus of the RhB dyes fluorescence.

Fig. 3(a) shows the spectra of a two stacked microdisks obtained with different power density. The diameters of two disks are 18 μm and 30 μm, respectively. It can be seen from Fig. 3(a) that when the power density is relatively low (i.e., 7.3 W/cm^2, 10.8 W/cm^2), only weak fluorescence exists. When the power density increases to a certain value (i.e., at $\sim$13 W/cm^2 for this specific structure), the lasing peak at $\sim$ 642 nm appears. As the power density further increases, the laser output increases rapidly, showing the lasing action. According to the Gauss fitting for the lasing line at 642 nm, the FWHM (full width at half maximum) of the lasing wavelength is only 0.25 nm, which corresponds to a Q-factor of 2600, which is far less than the actual value since the FWHM of the lasing line is comparable to the spectral resolution ($\sim$0.2 nm) of the spectrum that is determined by a He-Ne laser. Therefore the Q-factor of our device is much larger than that (a few hundreds) in the small disk in [11]. Furthermore, it can be clearly seen from Fig. 3(a) that the spectrum shows a single-mode lasing line with other modes suppressed greatly as compared with the spectrum shown in Fig. 2(e) reflecting the Vernier effect. Coupling strength is an important parameter for achievement of single-mode lasing. A systematic study on the effects of different disk parameters such as diameters, thickness, and relative positioning on the coupling strength will be conducted in the future.

To show the effect of the parameters of the fabricated microcavity on the lasing mode, we plot in Fig. 3(b) a multi-modes lasing spectrum obtained from a two stacked disks with the diameters of 36 μm and 60 μm. It can be seen from Fig. 3(b) that the peak intensities at 639.1 nm and 645.3 nm are stronger. This indicates that with the mode coupling and competition, modes at 639.1 nm and 645.3 nm are on resonance simultaneously for both disks. As a result, the FSR_{12} is about 6.2 nm which is five times larger than that of FSR_1 with the disk diameter of 60 μm, and three times larger than that of FSR_2 with the disk diameter of 36 μm. That is, $FSR_{12} = 5{*}FSR_1 = 3{*}FSR_2$. The result is in good agreement with the Vernier effect theory mentioned earlier, and further confirms that the coupling of the disks with Vernier effect leads to single mode lasing. Actually, the FSR of the stacked microdisks can also be affected by the disk materials with different refractive indices. For example, for the two stacked disks with $FSR_{12} = N_1FSR_1 = N_2FSR_2$, FSR1 or FSR2 is determined by the refractive indices of different materials according to $FSR = \lambda^2/\Delta n_{eff}L$, where λ is the lasing wavelength, L is the perimeter of the disk and $\Delta n_{eff} = n_1 - n_2$ is the effective refractive index of the disk. Therefore, it can be seen that the FSR of the coupled disks will be affected by both the diameter of the disks and the refractive index of the disk materials. The output laser intensity of the coupled disks also depends on the materials of the disks since different materials will give rise to different loss efficiencies due to, for example, different absorption or scattering.

It is known that finite difference time domain (FDTD) method can be ultilized to simulate the on-resonance wavelength, Q-factor, field distribution of any sophisticated structure, and thus we investigate the Vernier effect of two stacked disks (see the inset of Fig. 4(a)) by using FDTD method with Rsoft FULLWAVE. The spectrum analysis was performed by Pade approximation with Baker's algorithm [21], [22]. The diameters of the two microdisks in the simulation are 24 μm and 30 μm, respectively. The thicknesses of both microdisks are 1 μm. The xy plane is parallel to the surfaces of microdisks and the (0 0 0) position is set to be the center of the 30 μm microdisk located at the bottom (lower disk). Fig. 4(a) shows the simulated spectrum of the structure. For the wavelength at 622 nm that is on resonance with low loss, the energy in the upper disk and lower disk are mainly distributed at the periphery of the disks as shown in Fig. 4(b) and (c) respectively. The single mode filed distribution shown in Fig. 4b is inhomogeneous and it extends to the radial direction. This is the result of the superposition of multiple angular components caused by the asymmetric structure of the coupled microcavity. Fig. 4(d) shows the sectional view of energy distributions from the two disks with the cutting line (dash line) as shown in the inset of Fig. 4(a). It can be seen that at the overlapping edge (x = 0 μm, y = -15 μm)

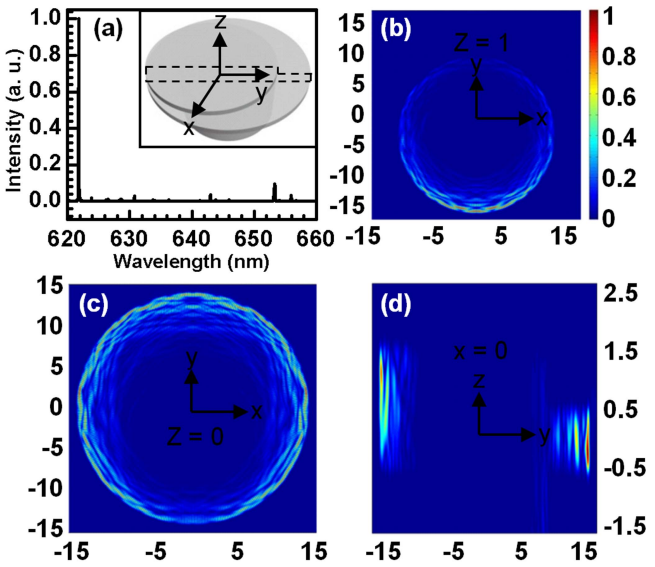

Fig. 4. The simulation of the single-mode laser. (a) The simulated spectrum of the laser shows single mode lasing. The inset shows the simulated structure. The electromagnetic field distribution in the smaller disk (b) and the larger disk (c) is shown. (d) is the electromagnetic field distribution of the section perpendicular to the disk. The axis units in (b)-(d) are μm.

of the two disks the energy has a strong distribution resulting from the coupling between two disks. Only a few frequencies can be on resonance in the coupled cavity (Fig. 4(a)) and with proper parameters single mode lasing can be achieved.

IV. Conclusion

In summary, we demonstrated the single-mode lasing from coupled WGM microdisks fabricated by the FsLDW technique. The realization of single-mode polymer PM microlaser was ascribed to the Vernier effect. The devices are only dozens of micrometers in lateral dimensions and several micrometers in longitudinal dimension. The fabricated size of the micro-devices could even be smaller depending on the designs, which guarantees the application of integrated optoelectronics.

References

[1] F. Vollmer and S. Arnold, "Whispering-gallery-mode biosensing: Label-free detection down to single molecules," *Nature Methods*, vol. 5, no. 7, pp. 591–596, Jul. 2008.

[2] T. Grossmann *et al.*, "Polymeric photonic molecule super-mode lasers on silicon," *Light, Sci. Appl.*, vol. 2, p. e82, Feb. 2013.

[3] A. M. Armani, R. P. Kulkarni, S. E. Fraser, R. C. Flagan, and K. J. Vahala, "Label-free, single-molecule detection with optical microcavities," *Science*, vol. 317, no. 5839, pp. 783–787, Jul. 2007.

[4] Y. Li, O. V. Svitelskiy, A. V. Maslov, D. Carnegie, E. Rafailov, and V. N. Astratov, "Giant resonant light forces in microspherical photonics," *Light, Sci. Appl.*, vol. 2. p. e64, Apr. 2013.

[5] K.-J. Che, Q.-F. Yao, Y.-Z. Huang, Z.-P. Cai, Y.-D. Yang, and Y. Du, "Multiple-port InP/InGaAsP square-resonator microlasers," *IEEE J. Sel. Topics Quantum Electron.*, vol. 17, no. 6, pp. 1656–1661, Nov./Dec. 2011.

[6] H.-H. Fang *et al.*, "Whispering-gallery mode lasing from patterned molecular single-crystalline microcavity array," *Laser Photon. Rev.*, vol. 7, no. 2, pp. 281–288, Mar. 2013.

[7] X. Fan, I. M. White, S. I. Shopova, H. Zhu, J. D. Suter, and Y. Sun, "Sensitive optical biosensors for unlabeled targets: A review," *Anal. Chem. Acta*, vol. 620, nos. 1–2, pp. 8–26, May 2008.

[8] J. Dai, C. X. Xu, and X. W. Sun, "ZnO-microrod/p-GaN heterostructured whispering-gallery-mode microlaser diodes," *Adv. Mater.*, vol. 23, no. 35, pp. 4115–4119, Sep. 2011.

[9] A. B. Matsko, A. A. Savchenkov, D. Strekalov, V. S. Ilchenko, and L. Maleki, "Review of applications of whispering-gallery mode resonators in photonics and nonlinear optics," *IPN Prog. Rep.*, vols. 42–162, pp. 1–51, Aug. 2005.

[10] X. Zhang, H. Li, X. Tu, X. Wu, L. Liu, and L. Xu, "Suppression and hopping of whispering gallery modes in multiple-ring-coupled microcavity lasers," *J. Opt. Soc. Amer. B*, vol. 28, no. 3, pp. 483–488, Mar. 2011.

[11] Q. Song, H. Cao, S. T. Ho, and G. S. Solomon, "Near-IR subwavelength microdisk lasers," *Appl. Phys. Lett.*, vol. 94, no. 6, p. 061109, Feb. 2009.

[12] X. Zhang, L. Ren, X. Wu, H. Li, L. Liu, and L. Xu, "Coupled optofluidic ring laser for ultrahigh-sensitive sensing," *Opt. Exp.*, vol. 19, no. 22, pp. 22242–22247, Oct. 2011.

[13] W. Lee, H. Li, J. D. Suter, K. Reddy, Y. Sun, and X. Fan, "Tunable single mode lasing from an on-chip optofluidic ring resonator laser," *Appl. Phys. Lett.*, vol. 98, no. 6, p. 061103, Feb. 2011.

[14] V. D. Ta, R. Chen, and H. Sun, "Coupled polymer microfiber lasers for single mode operation and enhanced refractive index sensing," *Adv. Opt. Mater.*, vol. 2, no. 3, pp. 220–225, Mar. 2014.

[15] L. Zhou, H.-H. You, and X.-Y. Pu, "Broadening free spectral range of an evanescent-wave pumped whispering-gallery-mode fibre laser by Vernier effect," *Opt. Commun.*, vol. 284, no. 13, pp. 3387–3390, Mar. 2008.

[16] H. Li, L. Shang, X. Tu, L. Liu, and L. Xu, "Coupling variation induced ultrasensitive label-free biosensing by using single mode coupled microcavity laser," *J. Amer. Chem. Soc.*, vol. 131, no. 46, pp. 16612–16613, Nov. 2009.

[17] S. Kawata, H.-B. Sun, T. Tanaka, and K. Takada, "Finer features for functional microdevices," *Nature*, vol. 412, pp. 697–698, Aug. 2001.

[18] B.-B. Xu *et al.*, "Flexible nanowiring of metal on nonplanar substrates by femtosecond-laser-induced electroless plating," *Small*, vol. 6, no. 16, pp. 1762–1766, Jul. 2010.

[19] J.-F. Ku, Q.-D. Chen, R. Zhang, and H.-B. Sun, "Whispering-gallery-mode microdisk lasers produced by femtosecond laser direct writing," *Opt. Lett.*, vol. 36, no. 15, pp. 2871–2873, Aug. 2011.

[20] Z.-P. Liu *et al.*, "Direct laser writing of whispering gallery microcavities by two-photon polymerization," *Appl. Phys. Lett.*, vol. 97, no. 21, p. 211105, Nov. 2010.

[21] Y.-Z. Huang and Y.-D. Yang, "Calculation of light delay for coupled microrings by FDTD technique and Padé approximation," *J. Opt. Soc. Amer. A*, vol. 26, no. 11, pp. 2419–2426, Nov. 2009.

[22] W.-H. Guo, W.-J. Li, and Y.-Z. Huang, "Computation of resonant frequencies and quality factors of cavities by FDTD technique and Padé approximation," *IEEE Microw. Wireless Compon. Lett.*, vol. 11, no. 5, pp. 223–225, May 2001.